*Traffic 2000* **1**: 614–621
*Munksgaard International Publishers*


*ISSN 1398-9219*

Toolbox

# How to Convert a Traditional Electron Microscopy Laboratory to Digital Imaging: Follow the 'Middle Road'

**John Heuser**

*Department of Cell Biology, Washington University School of Medicine, St. Louis, MO, USA*
*jheuser@cellbio.wustl.edu*

**Today, electron microscopy (EM) is increasingly confronted by the revolution in image-processing technology provoked by modern computers. Digital cameras are fast replacing film-based cameras in EM, as elsewhere, and the procedures for digital image-archiving, image-analysis, and image publication are rapidly evolving. To take advantage of these advances, we have chosen for the moment a 'middle road', in which film remains our basic recording medium in the electron microscope, but immediately thereafter, all film-based images are converted to digital files for further analysis and processing. The rationale behind this approach is that film still offers far greater sensitivity and resolution (providing an image equivalent to $>10000$ pixels per inch in a 1-s exposure), and film is still far easier to organize and archive than digital images of comparable resolution. However, digital manipulation of EM images has become mandatory. Hence, we explain here, in some detail, how we convert from film to digital.**

**Key words: Digital imaging, electron microscopy, resolution**

**Received 4 May 2000, revised 18 May 2000, accepted for publication 18 May 2000**

## Overview of the Following Essay

All electron microscopists are today facing the question of whether or not they should mount a digital camera in their electron microscope and stop taking electron micrographs on film. Here, we present our rationale for why we have not gone this route, despite the tremendous advances that have occurred in digital CCD cameras and the tremendous advances in computer–based acquisition of images from such CCD cameras. We will argue that the prudent course for at least the next few years will be to 'follow a middle road': namely, to continue to record EM images on $3.25 \times 4$ inch film while working at the electron microscope, but immediately thereafter convert these films to digital files for analysis and dissemination. We will indicate how this conversion to digital can be made rapidly and effectively, and in a manner that allows microscopists to confront their 'raw' data almost as freshly as they first confronted it during the initial microscope session. Additionally, we will explain how live TV viewing can be a tremendous aid at the time of first viewing samples in the EM. However, this is not for image acquisition, but rather for public display on a TV monitor so that others in the EM room (or others at great distances from the microscope, observing 'remotely' as has become the fad these days) can see for themselves the 'live' EM image—the image that heretofore was the private domain of the lone microscopist gazing intently at the dimly phosphorescent screen inside the electron microscope.

## Introduction to the Problems and Challenges Facing Microscopists Today

At issue today are basic questions of how best to 'handle' EM images: how to organize them by experiment and date, how to archive them for long-term storage and retrieval, how to analyze them and view them after the session in the microscope, how to handle them quantitatively, and ultimately, how to select, crop, and otherwise photographically manipulate them for final publication or other public dissemination. (Indeed, this final issue—of publication *vs.* other forms of public dissemination—is itself evolving rapidly these days.) Already, journals generally prefer to receive EM images as digital files, or go ahead and convert any submitted EMs to digital files themselves. Hence, it behooves all compulsive electron microscopists to generate their own digital files in a form that they consider to be optimal, just as earlier microscopists used to go into the darkroom and make their own 'very best prints' for publication. Furthermore, the whole new world of on-line publication, plus the advent of a variety of efficient protocols for image-dissemination and transfer directly over the Internet, has already changed the nature of scientific exchange at its very roots. This will increasingly affect the biomedical electron microscopist as well. In this world, digital files are a 'must', of course, and issues of how to convert EMs into an optimal form for general Internet dissemination intersect with issues of how to prepare digital EMs for more traditional publication in printed journals. Our opinion for how best to accomplish these separate but overlapping goals will be offered in this 'Toolbox' as well.

## Back to Basics: Why Stick with Film as the Primary Recording Medium for EM?

Basically, film still offers vastly greater sensitivity and resolution than CCD cameras. A simple way to appreciate this is to consider that standard EM film provides a resolution equivalent to roughly 10000 pixels per inch. (Note: since film is not a planar array of ~7 μm square photon-counting transistors that can be described as 'pixels', as is found on a CCD chip, but is instead a relatively 3-D layer of overlapping, light-sensitive, ~0.05 μm silver-halide crystals, its equivalency to 10000 pixels per inch may not be immediately obvious. The reader is referred to standard texts on photography published by Kodak, from which the Appendix provided at the end of this Toolbox has been exerpted.)

Accepting for the moment the notion that film offers a resolution of roughly 10000 pixels per inch, the second unassailable advantage of film is its sheer size: $3.25 \times 4$ inches in current usage. In comparison, the largest and highest-resolution CCDs currently available on the most advanced (and expensive) electron microscopes are roughly $2 \times 2$ inches in size and have roughly 2000 pixels per inch, yet these cost hundreds of thousands of dollars! The more typical CCD chips available at a 'moderate' cost for electron microscopes today are generally $1 \times 1$ inch and roughly 2000 pixels per inch. Comparing these various formats, we can see that one piece of sheet film creates an image equivalent to $32500 \times 40000$ pixels, or some 1300 megapixels, while the most expensive CCD chips create images of 16 megapixels and the standard CCD chips create images of roughly 4 megapixels (versus the oft-touted 1 or 2 megapixel chips in today's popular digital home cameras).

What these numbers mean in terms of effective resolution, which is of course what the electron microscopist cares about, will be discussed in detail in the next section. However, think first of these comparisons in terms of relative file-sizes. The 1300 MP image on a piece of film, even if recorded as a black-and-white image with only a moderate 8-bit of depth of contrast (256 grays) would be over 10 GB, larger than the entire hard drive of most current computers! Such an image would take probably an hour to 'open' in Photoshop and many hours to transfer on the even latest 100 MHz LAN Internet lines. By comparison, the highest-resolution digital images from the most expensive cameras would be roughly 128 MB, and the lower-resolution ones from more standard EM-type CCDs some 32 MB, only 1/300th of the file size provided by a single piece of film! (Even 30 years ago, Kodak was proud to boast that an entire 24-volume encyclopedia could be stored on a single photographic plate just 2.5 inches square.) These considerations indicate why film is, and will continue for some time to be, the optimal form of data-storage for information-packed images like electron micrographs.

## How Post-Magnification of Film Brings it Down to the Range of CCD Resolution

One caveat in the above comparison is that EMs are generally shot at lower than final magnification, e.g. final EM images are usually generated by photographic enlargement of the original EM negative (see Figures 1–3). A $3\times$ enlargement of an EM negative, typical for generating an $8 \times 10$ inch print, reduces its effective pixel size to 3000 pixels per inch, close to the range of current digital cameras, while a 10x enlargement (as is often used in single-particle analyses or as is used to make high-magnification 'insets' in published electron micrographs) reduces the film's effective pixel size to 1000 pixels per inch, well within the range of current digital cameras. (Still, the effective area of a 1000 pixel-per-inch CCD chip is only 1 or 2 inches square, while a 10x enlargement of an EM negative would create a 'mural' almost $3 \times 4$ feet across!) In any case, the clear advantage of film over CCD images becomes apparent when the microscopist goes to enlarge their image after the microscopy is done (see Figures 1–3).

Practically speaking, electron micrographs are rarely shot at greater than $100000\times$; more commonly, they are shot at $\sim 5000\times$. At $100000\times$, a single, ~20-nm macromolecule, would measure 2 mm on the final photographic negative. This 2 mm would be roughly 400 silver grains in diameter (assuming 10000 silver grains per inch; cf. Appendix, below). Hence, a 'standard' 2000 pixel per inch CCD in an EM could capture just as 'clear' an image of a 20-nm molecule if the primary microscope magnification was increased until the macromolecule filled roughly a quarter of the CCD chip. That would require projecting a 1 cm image of the molecule onto the CCD chip, which would require a primary microscope magnification something like 5 times higher than that used for film (e.g. around $500000\times$; derived from magnifying a 2-nm object to a 10-mm image). Indeed, modern electron microscopes are capable of achieving such high magnifications; but with even the brightest of electron guns the image is extremely dim at this point, and, hence, the duration of exposure (with even the most sensitive of current CCDs) would be several seconds—enough time for serious specimen drift, or even for frank physical deterioration of the sample from beam-damage. Still, even if one did manage to capture a digital image at $500000\times$, one would end up with a single 50–100 MB image of one molecule, versus an image of hundreds of molecules on a single $3.25 \times 4$ inch piece of film shot in 1 s at $50000\times$.

## When (and How) to do the Necessary Post-Magnification of Film

The moment for EM magnification to the molecular level is thus clearly not inside the electron microscope, but is, instead, later when post-processing the film. Here, to do this magnification, we strongly advocate the use of a top-end digital SLR camera (one with a 2–4 MP CCD chip) mounted on an old-fashioned photographic copy-stand. Devices such

as an old Bessler copy-stand, outfitted with a high-quality copy lens such as a Rodenstock 'Rodagon' and a bellows-type magnification tube, all mounted over a trans-illuminating base, allows one to enlarge an EM negative typically in the range of 3–10 × (Figure 4). Looking through the eyepiece of a quality digital SLR camera mounted on such a copy-stand provides the microscopist with a second 'primary' experience with their sample, much like the original experience of scanning the sample for good areas to photograph in the first place. Thus, he or she can search once again for good areas on the negatives, can appreciate structural contexts and interrelationships by eye, and then can select relevant areas for magnification and for instantaneous conversion to digital, just by a 'click of the shutter' on the SLR camera.

Black-and-white digital images from such cameras are typically imported via Firewire to a desktop PC as 5-10 MB TIFF files (or ~2 MB JPEG files, if so desired). As such, they are extremely easy to manipulate, catalog, store, transfer to other computers, etc. They become the microscopist's 'bread and butter': the images from which all further analysis and processing will be done. Perhaps dozens of such digital images can be shot from one single negative before the negative is 'retired' to an archival file. However, the EM negative will always remain available as a permanent, fully contextual record of the entire digital data-set.

## Why Convert to Digital with a SLR Camera Rather than a 'Flatbed' Scanner?

It is important to stress that we do not advocate 'scanning' EM negatives on modern flatbed scanners to obtain digital records of their entire contents (unless, of course, the microscopist simply wants to publish a 1× view of the entire negative). Again, this is because the file-size from a high-resolution scan of an EM negative (that is, a scan that would be sufficient to permit its later enlargement or cropping in Photoshop) rapidly becomes unwieldy. The typical maximum

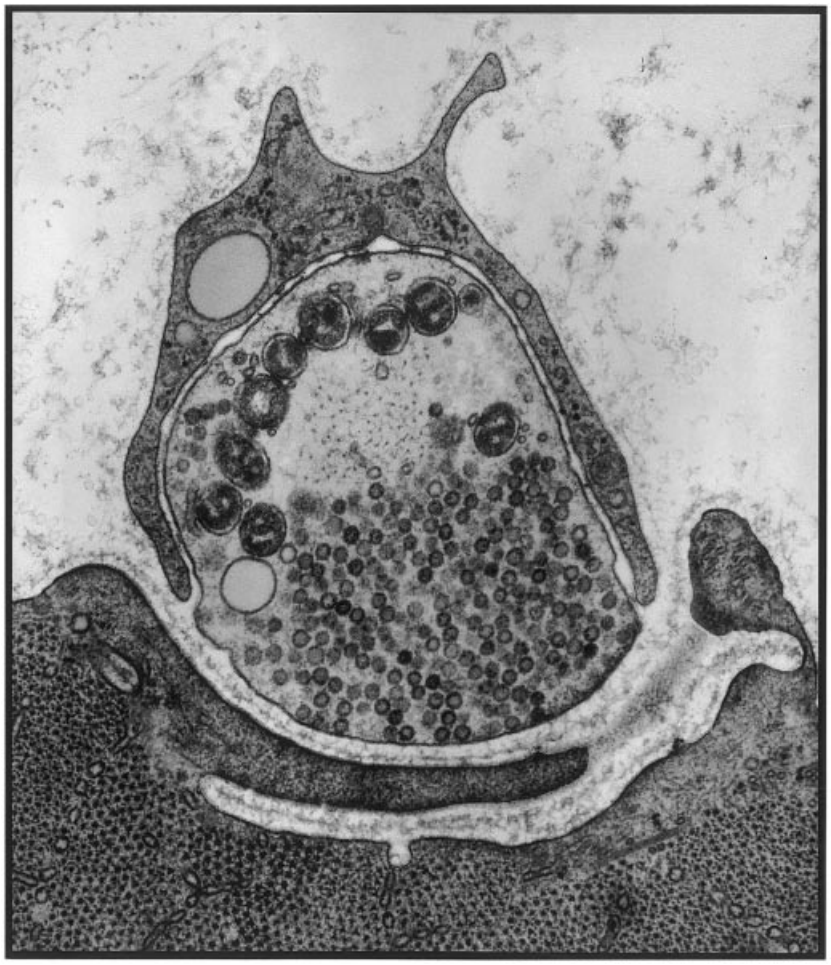

**Figure 1: A typical field of a routine electron micrograph.** In this instance, we see a 1.5 μm dia. nerve terminal filled with synaptic vesicles and mitochondria from a frog neuromuscular junction. This was originally shot at a primary magnification of 20000× in order to fill a standard 3.25 × 4 inch sheet of EM film. To generate this Figure, the original EM negative was contact-printed at 1× to fill the column. Comparable fields had to be shot on 1000 and 2000 pixel per inch CCD cameras at 6000x, due to their smaller 1 × 1 inch recording size. This made proper focusing of the image in the EM that much more difficult.

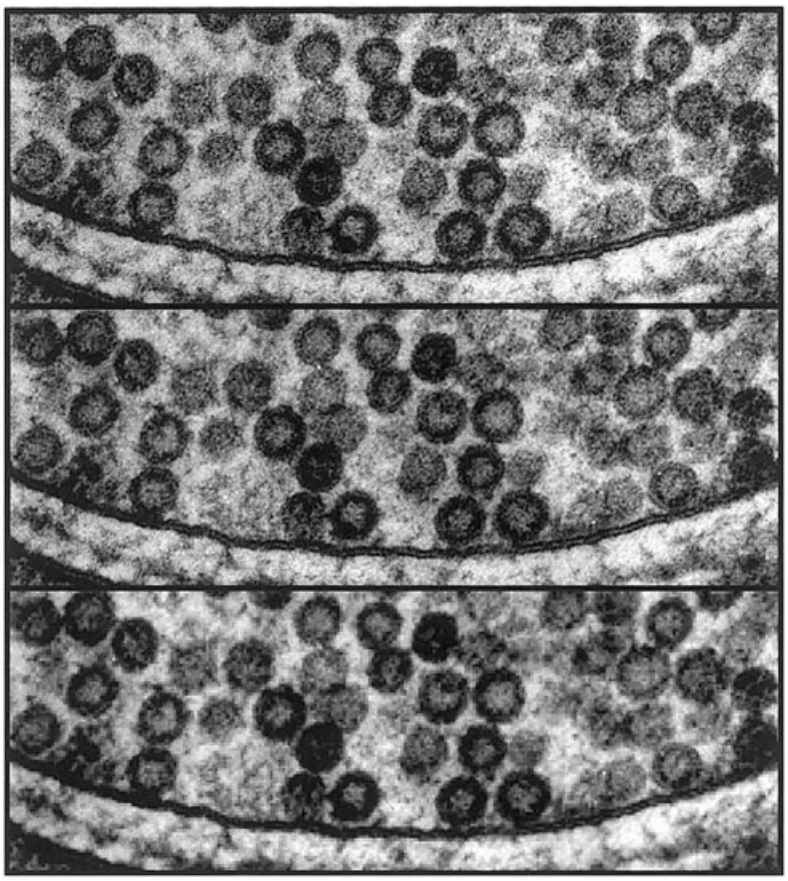

**Figure 2: Enlargements (3x) of the original film and CCD images shown in Fig. 1.** At this magnification, the loss in image quality in CCD images just begins to become apparent, mostly by the loss in clarity of cellular membranes. Top panel is the film image; center panel is a 2000 × 2000 pixel CCD image and lower panel is a 1000 × 1000 pixel CCD image.

flatbed scanning resolution of 1200 dpi will create a ~150 MB black-and-white file from a 3.25 × 4 inch negative, and will take at least several minutes to complete (versus the instantaneous 'click of the shutter' in the digital camera). In most desktop PCs, such a 150 MB file is opened rather slowly by Photoshop. (Furthermore, only four such files can be stored on an entire CD!) Even then, 1200 dpi file would permit selected fields to be taken from the negative and printed at no more than a 4× magnification (assuming the microscopist is trying to achieve the standard optimum for print resolution, which today is generally considered to be 300 dpi). But 4× is at the low end of the magnification range of the copy-stand/digital-SLR combination proposed above, and today's digital SLRs produce images that measure about 6 × 7 inches at 300 dpi, quite large enough for most journals (or measuring a whopping 2 × 2 ft at standard computer-screen resolution of 72 dpi). Hence, flatbed scanners are useful only for unmagnified conversions of EM negatives. At 300 dpi, a 1–2× flatbed scan of an EM negative creates a file in the range of 10–20 MB, comparable to the digital-SLR's image file-size.

## How to Handle Digital EM Files once they are Acquired

Once EM negatives have been converted from real film to digital files, a whole new world is opened, in terms of what can be done with them. We will not attempt to deal with this topic in any depth, except to say that the following computer-manipulations are basic to any 'digital' EM laboratory:

1. Photoshop® operations to manipulate the images.
2. A cataloging program such as Cumulus® or Extensis Portfolio® that will rapidly and seamlessly create 'thumbnails' of each and every image and catalog them (with storage and source-data that will make them instantly retrievable).
3. A CD-burning program such as Toast®, plus a CD burner to off-load the images from the computer as soon as experiments and data-sets are completed and image files are organized. (No amount of hard drive memory will suffice to store the vast numbers of digital images generated by the typical EM laboratory!) Indeed, we have 'burned' over 300 CDs filled with EM images in just the 3 years since we have converted to the 'middle of the road' approach advocated here. This is almost 200 GB of data.

(Of course, Kodak reminds us that this amount of data could theoretically be 'crunched' onto just 20 sheets of EM film!)

4. An Ethernet link and a visible Ethernet 'site', such as a homepage or an FTP site, where some (or all) of the digital EM files can be accessed, viewed by other investigators at remote sites, and if desired, downloaded to their own computers by a standard file-transfer protocols such as Fetch®. (Personally, we maintain a constantly available, public FTP site where EM images are 'mounted' for transfer to our colleagues during the active stages of a collaboration, or for transfer directly to journal publishers when a paper is ready for press. (Although we advocate this last link in the chain of working with digital EMs, we must admit that we have not properly addressed the potential problems of pre-publication publicity or copyright protection that free access to our images may be creating.)

## The Advantages of Converting to 'Live' TV Images While Working at the Microscope

Finally, although we eschew the capturing of 'primary' EM data by digital means for all the above reasons, we cannot stress strongly enough the great utility of creating live video images while one is actually sitting at the microscope. This not only eliminates the neck-strain and eye-strain of peering for long hours at the dimly phosphorescent screen through the dark porthole or through the binoculars of an EM, but—by bringing the image up to a nice, big, bright TV monitor—it allows colleagues and students of all ages to share the experience of EM viewing right as it is happening. Several people can sit in a room (or even at a great distance) and work together to scan a sample, to discuss what it represents, and to choose fields for photography. Indeed, the entire session can be videotaped for subsequent playback to others at a later time, allowing others to enjoy vicariously the original scanning and choosing (and more seriously, allowing

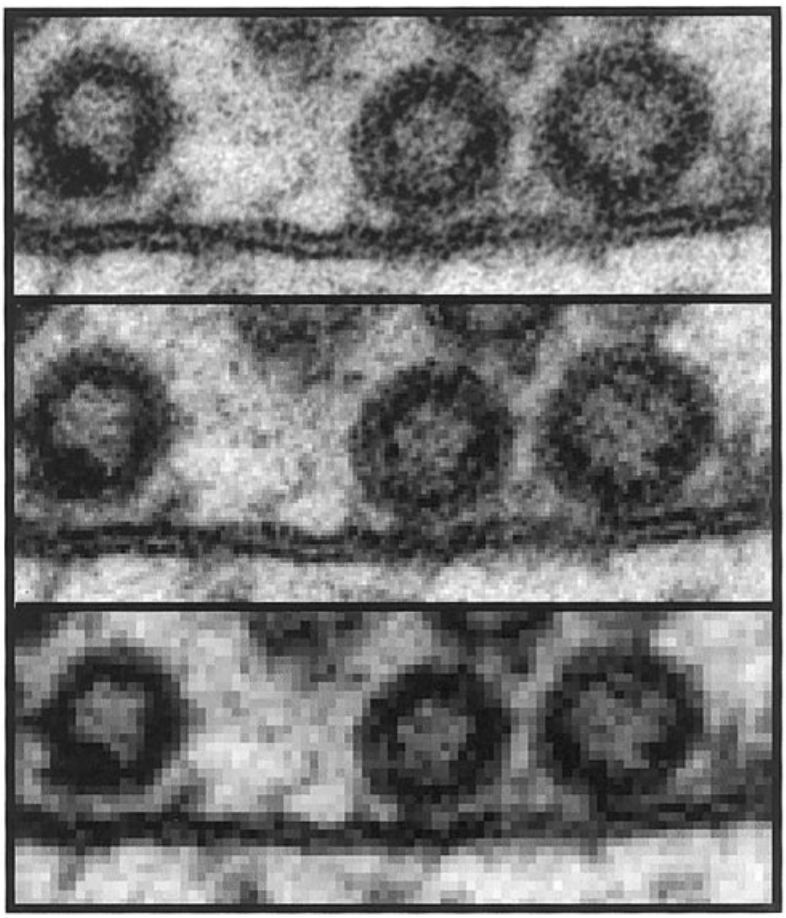

**Figure 3: Enlargements (3x) of the film and CCD images shown in Fig. 2.** At this magnification, the loss of image quality due to pixelation of the CCD images becomes immediately apparent. Indeed, the bilayer structure of the cell membrane is completely obscured in the 1000 × 1000 pixel CCD image at the bottom. In contrast, the film image at the top retains its full clarity with no apparent graininess even at this magnification.

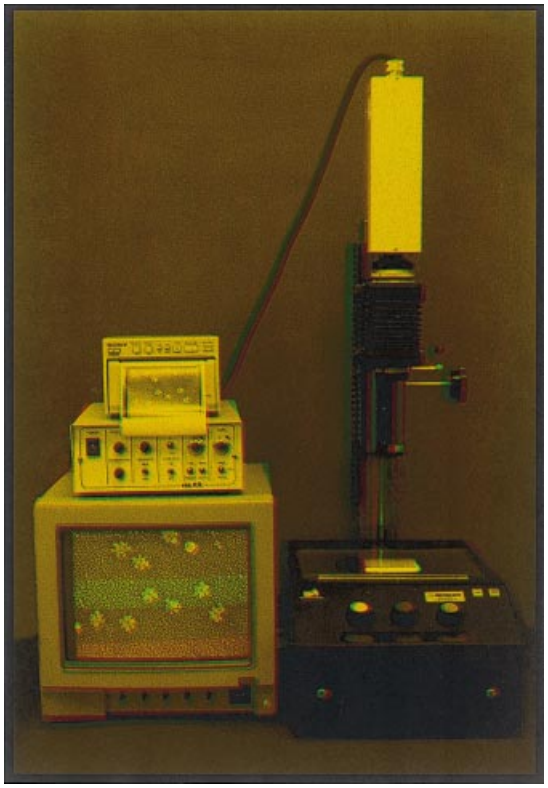

**Figure 4: Recommended copy-stand set-up for converting EM negatives to digital or TV files.** This is an anaglyph stereo image; see (1), for an explanation of this viewing procedure. (Anaglyph glasses available in Traffic 2000; 1) In the configuration shown here, images on EM film are converted to television for storage on optical memory disks and for instant generation of small prints with a Sony Model UP860 B&W thermal printer. For generation of computer-based digital files, the Newvicon camera and TV monitor shown here are substituted by a Kodak Professional DCS 520 SLR camera (the digital version of the Canon EOS-1 SLR camera), and images are imported instantly to a Macintosh G3 computer and monitor by a Firewire connection. Subsequently, digital images are printed with a Hewlett Packard Color 4500N LaserJet printer.

them to assess the overall condition of the sample and the degree of subjectivity that went into selecting the final image-choices, which has always been the biggest problem with electron microscopy). Our mentor, Sir Bernard Katz, once said publicly: 'If you look long enough in the electron microscope, you can find anything you wish.' (Actually, we don't fully agree with that dictum because there are plenty of things that we have 'wished' to find in the EM, but never could.)

A further advantage of substituting 'live' TV for direct viewing of the electron microscopic screen is that modern TV cameras are sufficiently sensitive that illumination levels can be kept very low, radiation damage to the sample can be minimized, and the microscope can be pushed to very high magnifications (or very thick samples can be viewed in energy-loss mode), when formerly, such samples would be too dim to see with the naked eye. (It is important to stress here that the actual resolution of these 'live' TV images or of the videotapes made of them is far too low for them to be a source of permanent still images.)

Here, we advocate the use of very standard analog (Newvicon) or digital CCD cameras with high sensitivity and good grayscale resolution, but only $640 \times 480$ resolution. These we suggest should be mounted external to the microscope and focused (via a standard 35 mm 'macro' lens from an SLR attached to the camera by a standard C-mount) directly through the porthole and onto the phosphorescent screen normally used for viewing. We have designed such a camera-mount so that it can be easily swung out of the way for direct viewing of the screen, when that is deemed necessary (Figures 5 and 6). Such a rig, including all its components—the camera, 35 mm lens, TV monitor, VCR, and some simple machined parts for the camera mount—should cost under $10000. Yet it totally obviates the need for an expensive internally mounted TV camera or a camera coupled by expensive fiber optics to a special screen inside the vacuum of the EM. Despite the fact that the true resolution of such TV images (or the videotapes of them) is far too low to be a source of decent still images, we do still attach a Sony thermal printer to our TV setup so that we can create little paper images that we can stick into our laboratory notebook. However, these serve as nothing more than thumbnail reminders of what we saw (c.f. Figure 4).

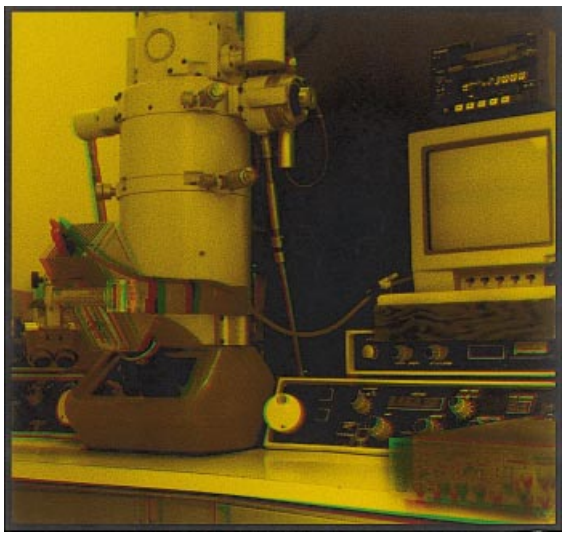

**Figure 5: Anaglyph stereo-view of TV equipment mounted on a standard JEOL 200CX electron microscope.** This set-up provides a TV monitor well-positioned for displaying the screen image to many viewers simultaneously, plus a control unit for live, real-time reversal of deep-etch EM images to 'negative contrast' for optimal depth perception, plus a digital video tape recorder for continuous acquisition of EM images as the sample is scanned. This tape deck can be connected by Firewire to a computer for storing low resolution 'thumbnail' images of areas worth further scrutiny and higher resolution film-based photography.

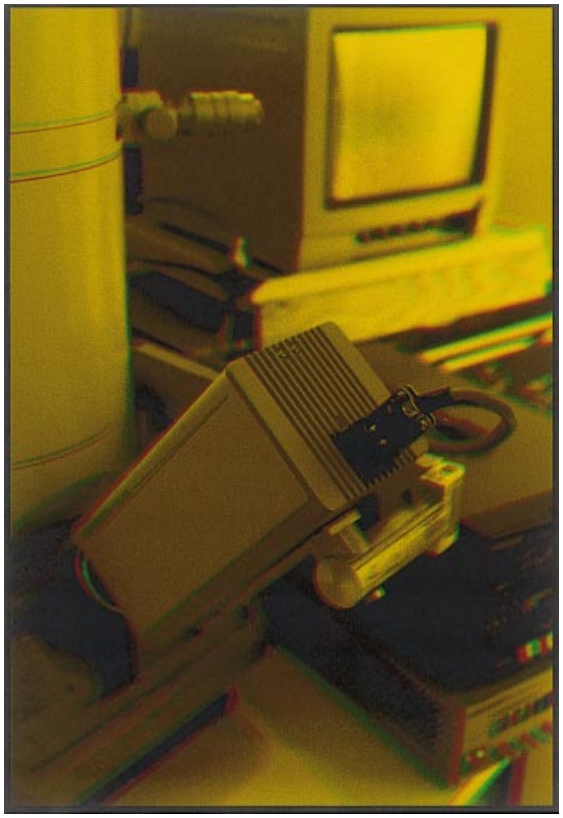

**Figure 6: Close-up anaglyph stereo-view of television camera mounting and positioning on the electron microscope.** A modern Hamamatsu 2400 Newvicon camera is aimed at the standard viewing screen of the electron microscope via a Nikon F1.4 35 mm focal length SLR camera lens coupled to it via a standard TV camera C-mount. The images provided by such cameras are far superior in gray scale and tone to standard EM-mounted CCD cameras, plus the camera is a fraction of the cost. The camera can be swung out of the way for normal viewing of the EM screen via the simple hinged arm visible immediately below it. This can be easily constructed in any University machine shop from plain aluminum.

## 'Live' TV Contrast-Reversal for EM Laboratories that do Freeze-Etching

The final advantage of 'live' TV viewing for EM laboratories that do freeze-etch microscopy, in particular, is that the TV-rendering allows a contrast-reversed image to be presented on the TV monitor, right during the actual observation period. We have long advocated contrast-reversal for freeze-etched and platinum-replicated samples, simply because it makes the platinum-coated elevations of the sample look 'highlighted' (rather than dark as they appear on the screen, since platinum is the electron-scattering part of the sample) and it makes the non-platinized 'depths' of the sample look dark, as if they were truly 'in the shadows'. This greatly assists the viewers' ability to discern the correct 3-D topology of a sample, right while they are viewing it. Formerly, this had to be performed by making contact-printed inter-negatives of each and every plate shot in the electron microscope, and then by printing these inter-negatives on photographic paper: a highly laborious and expensive process. Now, this can be performed by a direct 'contrast reversal' in Photoshop (although the digital SLR enlargements advocated above are made directly from the EM negatives, so they are already contrast-reversed).

In any case, doing a contrast-reversal 'live', right while several people are viewing a platinized sample together, greatly assists the microscopist to share with others the wonderful experience of 'the search'. This is what makes electron microscopy such a fun 'distraction,' as Keith Porter used to call it.

## Acknowledgments

Hearty thanks to several outstanding electron microscopists who reviewed and provided valuable advice on the above Toolbox. These included Ken Downing of the Lawrence Berkeley Laboratory, David DeRosier of Brandeis University, Edward Egelman of the University of Virginia, and Joachim Frank of the Wadsworth Institute in Albany.

## References

1. Heuser JE. Membrane traffic in the anaglyph stereo. Traffic 2000;1: 35–37.

## Appendix A

The statement that EM film resolution approximates 10000 dpi implies that it has an effective resolution (or grain size) of ~3 μm. Of course, a developed black-and-white photographic image consists of silver particles suspended in gelatin. The size and distribution of these particles, together with the thickness of the emulsion layer, contribute to the image-structure properties of any given film. However, in describing these properties, the terms 'granularity', 'resolution', 'sharpness', etc., etc. can be very confusing and misleading. To help the reader think more clearly about these matters, the following statements have been exerpted and paraphrased from old Kodak publications. Some of these old publications plus more current explanations of film characteristics can be obtained from Silver Pixel Press, 21 Jet View Drive, Rochester, NY 14624. Their website address is: http://www.saundersphoto.com/html/books.htm

***'Granularity'***

While the densities in a photographic film may appear to the eye to be homogeneous, microscopic examination will reveal a collection of discrete particles of metallic silver. These 'grains' form a pattern that becomes visible when a photographic image is enlarged. Two terms are used to refer to this pattern: 'graininess' and 'granularity': 'graininess' is the subjective impression of it, while 'granularity' is a true objective measure of it (typically obtained by scanning film with a microdensitometer having a 48 μm circular measuring aperture).

***'Resolving power'***

Resolving power refers to the ability of a film to record distinct images of small, nearly contiguous objects in a scene (cf. 'American National Standard Method for Determining the Resolving Power of Photographic Materials,' PH2.33-1969). Typically, this is defined as a film's ability to maintain separate images of parallel bars whose relative displacement is very small, which is generally described in lines/mm.

Importantly, the resolving power of film is a function of the relative contrast of the parallel bars or 'target elements' used in a resolution test-pattern. It also depends upon a number of other factors. In general, the higher the contrast of the film, the higher its resolving power. (This is simply because higher contrast films are finer-grained.) Resolving power is also affected by exposure, peaking at a certain optimum exposure level and then falling off at higher levels, largely due to diffusion or scatter of light within the photographic emulsion. In addition, processing conditions and different types of developer can exert a measurable effect on resolving power.

***'Modulation transfer characteristics'***

The 'Modulation Transfer Function' (MTF) describes the ability of a film to more or less accurately reproduce varying inputs of light, as a function of spatial frequency. It specifically measures the effects of light scatter in the emulsion during exposure and the chemical dynamics that occur during the development process. To measure the MTF, patterns with sinusoidal variation in luminance are projected onto film. The spatial frequencies of these sinusoidal patterns extend from well below to well beyond the maximum resolving-power of the film, though generally do not exceed 400 cycles/mm.

During exposure, scattering within the emulsion results in a reduction in the image modulation, which is increasingly obvious at higher spatial frequencies. This can be quantitated by scanning the processed photographic image with a micro-densitometer. The ratio of the actual modulation of densities in the film, compared to the original optical image projected onto the emulsion, is called the 'modulation transfer factor.' Plotting this factor as a function of spatial frequency (expressed in cycles per millimeter) results in an MTF curve. The Fourier transform of such an MTF curve represents the 'spread function' of the film, the most objective value of its image-capturing characteristics.

Although emulsion-scattering and film-processing effects combine with grain size to determine both the MTF and resolving power of any film, these two measures of are not numerically related. For this reason, it is not possible to determine classical resolving power (in lines/mm) by simply identifying the spatial frequency (in cycles/mm) at which the MTF drops to some arbitrary response, e.g. 5%. The published resolving powers of two different films might well be identical, but their imaging properties could still be very different. Resolving power is a function of the granularity and 'micro-densitometry' of a film as well as its MTF. More detailed information and help in working with the MTF (sine-wave response) of film can be found in numerous technical papers referenced in the SPSE Handbook of Photographic Science and Engineering.

***'Sharpness'***

Although resolving power is a measure of the ultimate ability of a photographic material to record fine detail such as double-stars or fine parallel lines, it is often not the most important factor in microscopy. Generally of more importance is the 'sharpness' with which an image is reproduced. Although resolving power is one important indication of a film's ability to produce 'sharp' pictures; it does not follow that a series of photographs will necessarily be ranked in the same order for 'sharpness' as for resolving power. By using certain combinations of lenses and films, it is possible to make two photographs, one of which has a higher resolving power but a lower 'sharpness' than the other. Moreover, some developers reduce 'sharpness' markedly while affecting resolving power very little.

The resolving power versus 'sharpness' of a photographic material are conditioned primarily by two factors: the turbidity and the inherent contrast of the emulsion. First, considering the turbidity of an emulsion, it is a product of two conflicting variables: its light-scattering power versus its light-absorbing power. Turbidity is measured as follows: when a film is exposed to an image of a point or an extremely narrow line in a series of increasing doses, image size increases with increasing exposure level, and does so at a rate that directly reflects emulsion turbidity. Second, the inherent contrast of an emulsion depends primarily upon the range of grain sizes and grain shapes within it. Like turbidity, these film characteristics are fixed by the method of manufacture. On the other hand, the contrast and 'sharpness' of a particular image can be altered drastically by varying its development conditions, although this generally exerts only a minor influence upon its actual resolving power.

*Journal of Microscopy, Vol. 200, Pt 1, October 2000, pp. 1–13.*
*Received 7 March 2000; accepted 6 June 2000*

INVITED REVIEW

# Digital imaging in transmission electron microscopy

G. Y. FAN & M. H. ELLISMAN
*National Center for Microscopy and Imaging Research, Department of Neurosciences, School of Medicine, University of California, San Diego, La Jolla, CA 92093, U.S.A.*

**Key words.** ASIC, CCD camera, electron scintillator, imaging plate, TEM.

## Summary

The digital revolution currently under way, as evidenced by the rapid development of the Internet and the world-wide-web technologies, is undoubtedly impacting the field of transmission electron microscopy (TEM). Digital imaging systems based on charge-coupled device (CCD) technologies, with pixel array size up to 2 k × 2 k at the present and increasing, are available for TEM applications and offer many attractions. Is it time to phase out film cameras on TEMs and close the darkrooms for good? This paper reviews digital imaging technologies for TEM at different voltages, and contrasts the performance of digital imaging systems with that of TEM film. The performance characteristics of CCD-based digital imaging systems, as well as methods for assessing them, are discussed. Other approaches to digital imaging are also briefly reviewed.

## 1. Introduction

Charge-coupled devices (CCDs) were invented in 1970 (Boyle & Smith, 1970). They soon became the sensor of choice in many imaging applications, particularly in video cameras and camcorders. However, a large driving force behind the development of large format CCDs, with array size greater than 1 k × 1 k, came from astronomy imaging, particularly in space-borne observatories, where high resolution images were needed but it was impractical or impossible to use photographic film, as in the well-known example of the Hubble Space Telescope. The instant image access in electronic form, high sensitivity and extremely low noise offered by cooled CCD sensors makes them ideal for astronomy applications. Experimental CCD imaging systems for telescopes were built as early as 1976, and large format CCD imaging systems are in wide use today.

Correspondence: Gary Fan. Tel: +1 619 534 5637; fax: +1 619 534 7497; e-mail: gfan@ucsd.edu

In transmission electron microscopy (TEM), however, there had been a considerable delay for the adaptation of CCD technologies. The first experimental digital imaging system for TEM based on the CCD technology was reported in 1982 (Roberts *et al.*, 1982), in which a 100 × 100 pixel CCD was directly exposed to 100 keV electrons. Six years later, Spence & Zuo (1988) reported a 576 × 382 pixel CCD imaging system which used an indirect detection scheme, involving an electron scintillator screen and an optical coupler, which avoided some of the problems encountered in the direct detection design. Many more experimental systems have since been reported and research effort in this direction continues until this day (Aikens *et al.*, 1989; Chapman *et al.*, 1989; Daberkow *et al.*, 1991; Krivanek *et al.*, 1991; Herrmann & Liu, 1992; Kujawa & Krahl, 1992; Fan & Ellisman, 1993; Krivanek & Mooney, 1993; Faruqi *et al.*, 1995; Herrmann & Sikeler, 1995; Daberkow *et al.*, 1996; Downing & Hendrickson, 1999; Fan *et al.*, 2000). These systems and the commercial digital imaging systems specifically designed for TEM, which became available in the early 1990s, have been successfully used in many applications that are difficult or impossible to carry out without an online digital imaging system, including microscope auto-tuning (Krivanek & Fan, 1992), automated electron tomography (Dierksen *et al.*, 1992; Koster & de Ruijter, 1992; Koster *et al.*, 1992), electron holography (Daberkow *et al.*, 1996; Duan *et al.*, 1998), protein electron crystallography (Brink & Chiu, 1994; Downing & Hendrickson, 1999; Faruqi *et al.*, 1999) and telemicroscopy (Fan *et al.*, 1993; Voelkl *et al.*, 1997).

Despite the many advantages offered by CCD-based imaging systems, and despite the rapid development in and wide use of digital technologies in recent years, the transition from film recording to digital imaging in the field of TEM proves to be a slow process. At present, new TEMs are shipped with a film camera as the standard equipment, as they had been for more than half a century, except that 1 k × 1 k or 2 k × 2 k CCD cameras are now offered as

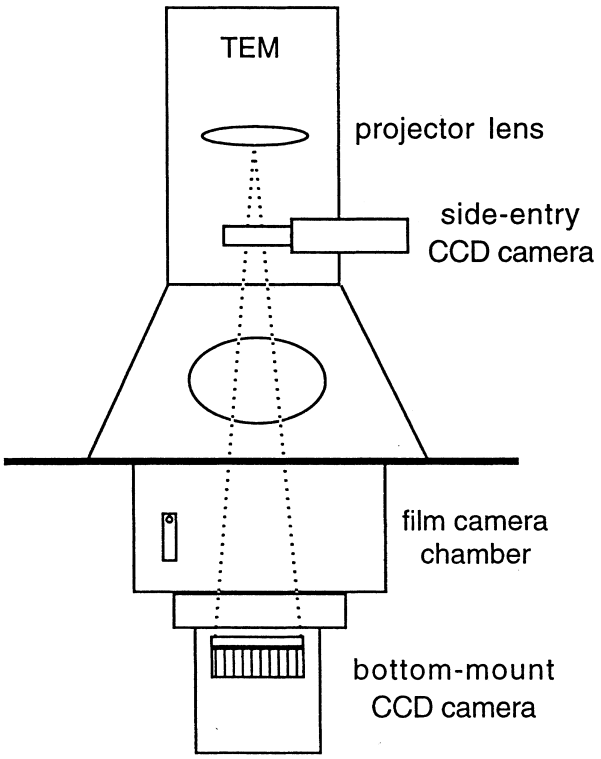


**Fig. 1.** CCD digital imaging systems for TEM are available for both side-mount and bottom-mount positions. These systems typically consist of a 1 k × 1 k or 2 k × 2 k CCD sensor and operate under slow-scan mode, with a readout speed of several frames $s^{-1}$ at the most. Video-rate systems are also available, but they have smaller format, and are useful for searching and focusing purposes. The extremely large depth of focus of transmission electron microscopes can form focused images at both detector positions simultaneously. However, the difference in the distance from the last beam crossover point results in a significant change in magnification in the images.

third party add-ons (Fig. 1). This relatively slow pace of adaptation reflects partially the satisfactory performance, at least in some importance aspects, of film recording in TEM under a wide range of electron energies and the difficulty of using CCDs for imaging with high energy electrons, as will be discussed below. More important, however, is the limited number of pixels offered by the currently available systems, as compared with that obtained by digitizing a TEM negative (Fig. 2). Even so, given the many attractions offered by digital imaging, it seems inevitable that film recording in TEM will eventually be replaced by CCD-based or other emerging digital imaging technologies.

## 2. Principles of CCD imaging

The principle of CCD operation (see, e.g. Theuwissen, 1995) is schematically illustrated in Fig. 3. When a photon or other type of ionizing particle enters the CCD, one or more electron–hole pairs may be created in the silicon substrate, depending on the energy of the incident particle. However, due to reflection and other energy competing processes in the substrate, a photon may not create an electron–hole pair even if it has enough energy to do so. The fraction that does is called the quantum efficiency of the CCD. This is an important parameter and is a function of the wavelength of the incident photons (Fig. 4). Its peak value varies from 12% in the consumer grade CCDs to better than 90% in scientific grade CCDs. Electron–hole pairs are also created in CCDs due to thermal excitations, causing dark noise in the CCD. Dark noise accumulates with time, but can be reduced by cooling the CCD. Dark noise reduces by 50% for every ~7 °C drop in temperature in silicon. At − 30 °C, dark noise can be reduced to a level of a few electron–hole pairs per pixel per second in a CCD.

Electrons generated in a pixel are collected in the potential well during integration (Fig. 3a). The amount of charge accumulated in a pixel is therefore proportional to the number of photons incident on that pixel during the period of integration. By coordinating the gate voltages (Fig. 3b), charges in one pixel can be transferred to an adjacent pixel, or any other pixel in a stepwise fashion. Typically, charges in any pixel have a fixed pathway to a readout register where the charge can be amplified and digitized. The number of transfers along the pathway will of course depend on the relative position of the pixel to the readout register, and the largest will be ~M + N for a M × N device. Due to the large number of transfers, particularly in large array CCDs, the charge transfer efficiency has to be very high to avoid charge loss. For scientific grade CCDs, the charge transfer efficiency reaches ~0.99999. Even so, it can be calculated that the charge loss can be as high as 4% for some pixels in for a 2 k × 2 k CCD.

During charge transfer, a shutter is typically used to prevent photons reaching the CCD, which would otherwise cause image smearing. For applications where a mechanical shutter is impractical, as in video rate or other high frame rate imaging systems, special CCD designs have been developed, such as the interline- and frame-transfer CCDs (Fig. 5). These special designs serve as electronic shutters, which reduce image smearing to a minimum level. A trade-off is that there will be some dead areas for interline-transfer CCDs, which reduce their sensitivity, whereas the frame-transfer design has a pixel array utilization of only 50%.

## 3. CCD imaging in TEM

As ionizing particles, electrons with enough energy can also create electron–hole pairs in a CCD. Thus, CCDs can also be used for direct electron imaging. However, given the average pair-production energy of 3.64 eV in silicon (Fiebiger & Muller, 1972), one incident electron generally creates too many electron–hole pairs in a CCD given the energy range

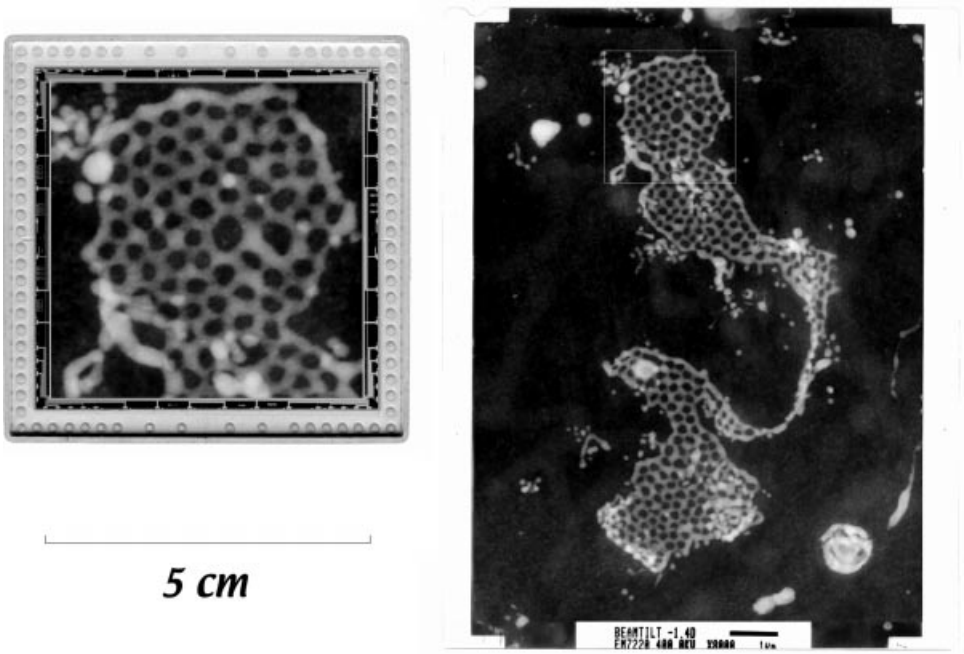


**Fig. 2.** A 2 k × 2 k CCD sensor (left) and a TEM negative film (right). The CCD (SITe SI424A) has a pixel size of 24 μm × 24 μm, and an imaging area of ~5 cm × 5 cm. The film (Kodak electron microscope film 4489) has an imaging area of ~7 cm × 9 cm. Because of the resolution difference, the CCD captures a smaller image area than its physical size suggests. The box on the negative shows the approximate area, as schematically overlaid on the CCD, that can be captured by the CCD if images are to be sampled at the same resolution. The specimen is a 1 μm section of selectively stained frog ganglia, showing the cis-face of the Golgi apparatus, taken at 400 kV.

typically involved in TEM. For example, a 100 keV electron will create in the order of 27 k electron–hole pairs in silicon, assuming the pair-production energy of 3.64 eV is valid for 100 keV electrons. A 24 μm × 24 μm CCD pixel, which is the largest pixel size in use at the present, can have a full well capacity as high as ~500 k well electrons, whereas a 15 μm × 15 μm pixel has only about 80 k. Therefore, direct detection would result in an imaging system with a very high sensitivity but a very low dynamic range. The first experimental direct detection system by Roberts and co-workers (Roberts *et al.*, 1982) reported a saturation level of 45 incident electrons at 100 keV. At higher electron energies, the dynamic range will be even lower. More importantly, the radiation damage to the CCD by the energetic electrons is a serious problem even at 100 keV, which changes the CCD imaging characteristics markedly as a function of cumulative electron dose on the CCD (Roberts *et al.*, 1982).

To avoid these problems, current CCD imaging systems for TEM applications invariably employ a scintillator screen, which converts an electron image to a photon image (Fig. 6). The photon image is then relayed to the CCD sensor either by a fibre-optic coupler or a lens.

This indirect detection scheme works well in circumventing the problems mentioned above, but unfortunately also introduces some new ones. First is the scintillator itself,

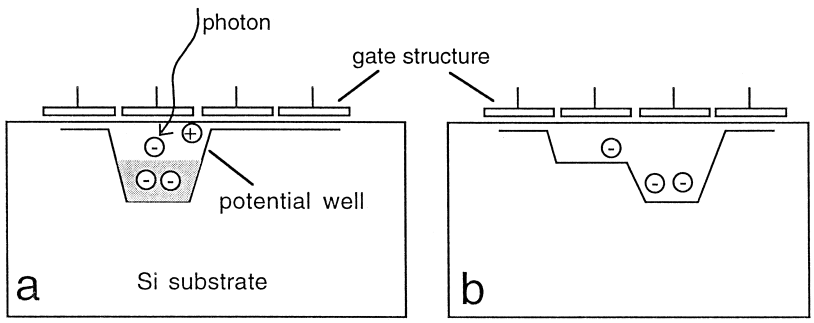


**Fig. 3.** Schematic illustration of CCD structure and operation. Front-side illuminated CCD is shown. In such a device, a photon must penetrate the electronic gate structure before it can interact with the Si substrate. The device can also be flipped over, the Si substrate thinned and anti-reflection coated to create a back-side-illuminated CCD, which has a considerably higher sensitivity.

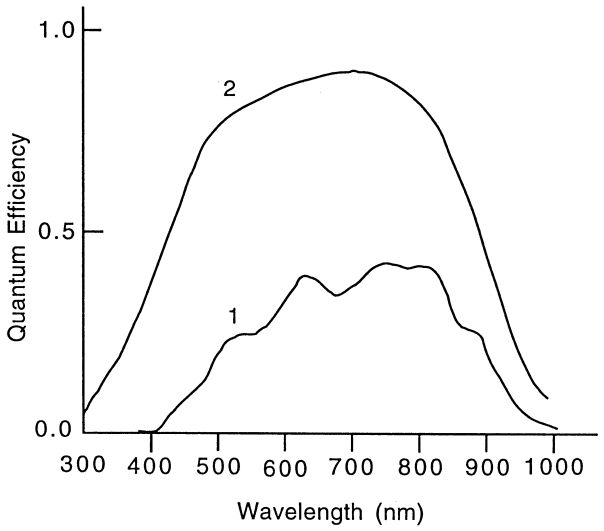


**Fig. 4.** Typical quantum efficiency curves of front-side-illuminated (1) and back-side-illuminated, anti-reflection-coated (2) scientific grade CCDs. An improvement in sensitivity by a factor of two can be easily achieved with the back-side-illuminated CCDs.

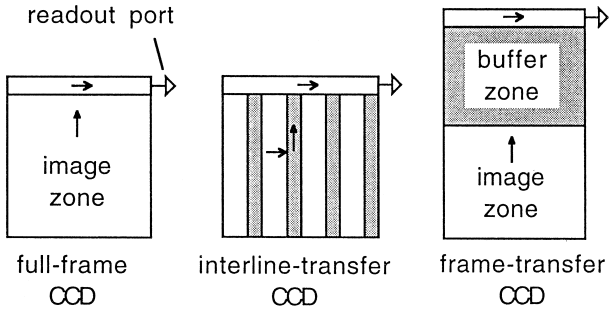


**Fig. 5.** Schematics of full-frame, interline-transfer and frame-transfer CCDs. The latter two types are used in fast rate imaging systems. Arrows indicate directions of charge transfer. Shaded areas are light-shielded.

which may have a low photon yield, and/or a large point-spread function. The relay optics may further impose a resolution limit, relay efficiency, shading and geometrical distortion. These are discussed below.

### *3.1. Electron scintillator screens*

At present, the resolution of a CCD imaging system for TEM is limited to a large degree by the scintillator screen used. Figure 7 gives some Monte Carlo simulations (see, Joy, 1988; Russ *et al.*, 1990; Meyer & Kirkland, 1998) of electron scattering and photon generation in a scintillator material, crystalline yttrium aluminium garnet (YAG), at different electron energies. As expected, the dimension of the point-spread function increases drastically with electron energy. Even at 100 keV, the diameter of the point-spread function is in the order of 50 μm, whereas the pixel size of large format CCDs useful for electron microscopy is 24 μm or smaller. This means that the point spread function of the scintillator will cover several CCD pixels, therefore reducing the effective array size of the CCD. For example, a 1 k × 1 k CCD may only provide 500 × 500 independent pixels. The situation worsens rapidly with increasing energies.

Two remedies are apparent for this large point-spread function problem: (1) using a thinner scintillator screen, and (2) using a reducing optical relay. Both, however, lower the sensitivity of the imaging system.

With a thinner screen, an incident electron may go through the scintillator before depositing an appreciable fraction of its energy, hence reducing the number of photons generated. In addition, this method is less effective when the scintillator screen has a support substrate such as a glass or fibre optic plate, because the substrate will backscatter a fraction of the incident electrons which may re-enter the scintillator, thus increasing the point-spread function. This is a more serious problem at higher electron energies. Monte Carlo simulations done by Meyer & Kirkland (1998) show that the re-entry rates are 0, 16, 22 and 25% for

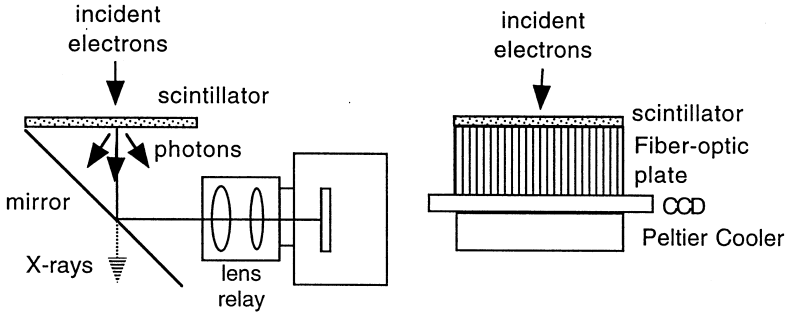


**Fig. 6.** CCD cameras in TEM. Instead of direct detection, a scintillator screen is used to convert an electron image to a photon image which is relayed, via a lens or an optical fibre plate, to a CCD. A bending of the optical path by 90° in the lens coupled system has the advantage of preventing X-rays from hitting the CCD, which would otherwise create bright spots on images. As the CCD sensor is cooled to ~ − 30 °C to reduce thermal noise, it has to be in a vacuum to avoid ice formation.

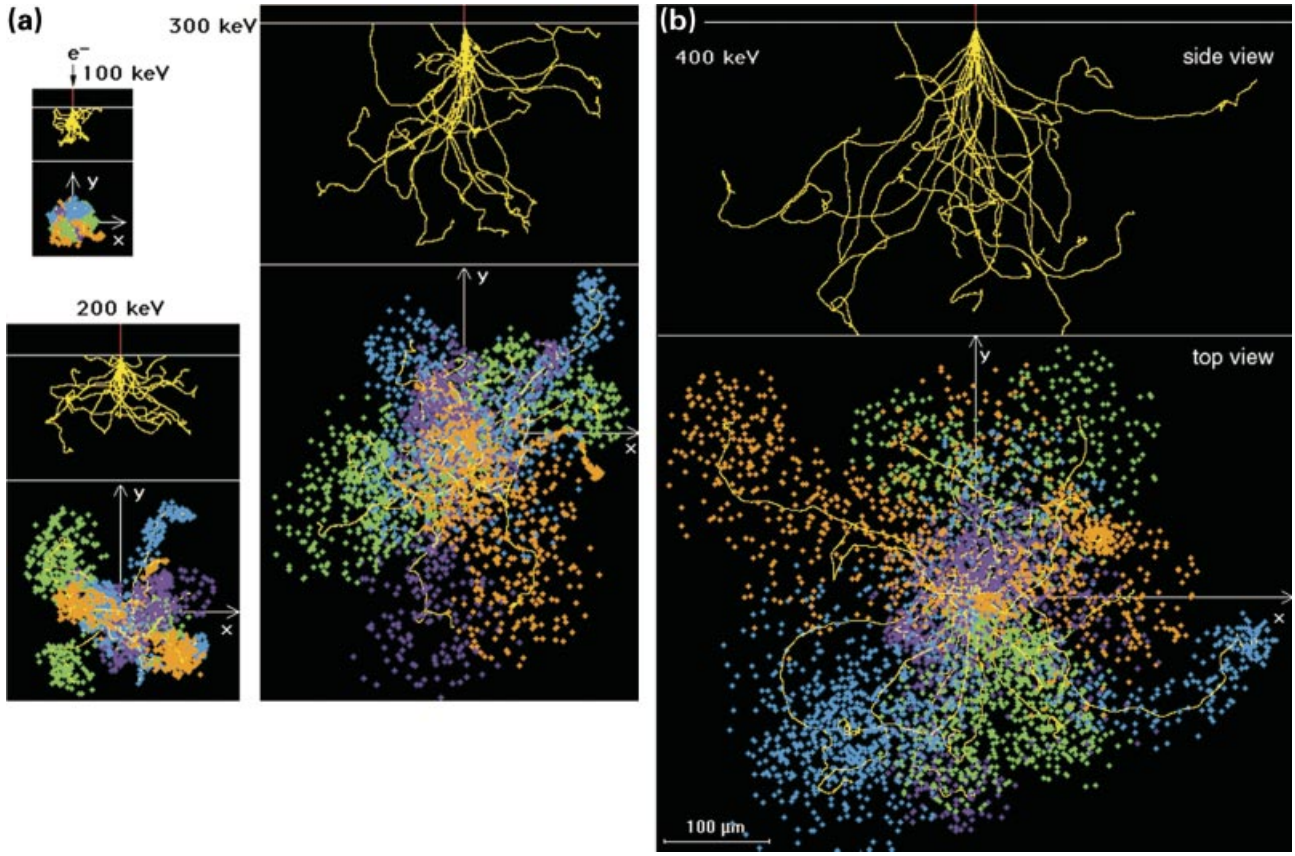


**Fig. 7.** Monte Carlo simulations of electron scattering (side views) and photon generation (top views) in crystalline YAG at different electron energies as marked. In each case the trajectories of 20 incident electrons are shown. In the top views, photons due to each incident electron and its secondary electrons are colour coded. The point-spread function in the scintillator increases rapidly with electron energy, making it necessary to use thin scintillator screens for high voltage imaging applications to avoid resolution loss. In polycrystalline scintillators, such as powder phosphors, further scattering of photons is significant and will worsen the point-spread function even more. (The computer program used for the simulations was from Meyer & Kirkland (1998), and can be found online at www-hrem.msm.cam.ac.uk/~rrm/mc.html)

electron energies of 100, 200 300 and 400 keV, respectively, for a 50 μm YAG layer on a thick $SiO_2$ support.

The brightness of a scintillator screen is another important parameter of a TEM imaging system as it has a direct impact on the sensitivity of the imaging system. It depends on the scintillating material from which the screen is made, the amount, or the thickness, of the scintillating material used, the way the screen is constructed, and the electron energy for which the screen is used. Two commonly used types of scintillating materials in TEM imaging are powder phosphors and single crystal YAG. Powder phosphor screens are generally much brighter than YAG screens, but are not as uniform (Daberkow *et al.*, 1991). Also, a single crystal YAG is transparent to light, whereas powder phosphor is fairly opaque and highly scattering. As a result, only photons generated near the exit surface of a phosphor screen are useful for image formation. Therefore, too thick a layer of phosphor may not only degrade the screen resolution but lower screen brightness as well (Fan & Ellisman, 1996). The thickness of the phosphor layer should be optimized for the electron energy for which the screen is used. Figure 8 gives the relative brightness of P20 phosphor screens as a function of electron energy, and should provide some guidelines when deciding the phosphor layer thickness to be used.

### *3.2. Optical relay*

With a reducing optical relay, obviously the point-spread function will be reduced proportionally when it is relayed to a CCD sensor. The trade-off is that the light collection efficiency of the relay goes down with the square of the reduction factor. This is true when using either a reduction lens relay or fibre-optic taper, but it is easier to understand in the case of a lens relay: to achieve a greater reduction, the lens will have to be moved further away from the screen. For a self-illuminating object that has an isotropic luminescence, as is the case for scintillating screens, photon flux falls off with the square of the distance between the lens and the object.

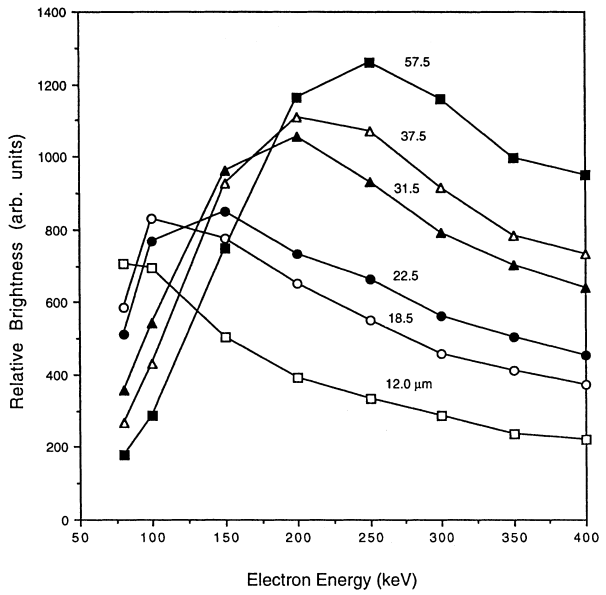


**Fig. 8.** Relative brightness of phosphor screens of varying thickness (labelled in μm) as a function of incident electron energy (from Fan & Ellisman, 1996).

The relative merits of fibre-optical and lens coupling have been discussed by various authors in the literature. Generally speaking, a fibre-optical coupler offers a much higher collection efficiency (~20%) and a compact design. A lens relay provides more flexibility and allows for the use of a thin-foil screen, therefore it can provide a better resolution, particularly at higher electron energies. The choice as to which one to use will depend on microscope accelerating voltage and other system requirements.

At electron energies of ~100 keV and below, as the difference between the point-spread functions in scintillating screens with and without a substrate is not significant, the higher collection efficiency and a compact design offered by fibre-optic coupling make it a more attractive choice, whereas at high electron energies, particularly at 300 keV and above, the point-spread function in screens with a substrate becomes too large to be acceptable. Downing & Hendrickson (1999) recently reported that a 2 k × 2 k fibre-optic coupled imaging system, which has a CCD with 24 μm square pixels and a 1 : 1 fibre-optic coupling plate, should be used in 2 × 2 binning mode at 400 keV due to the large point-spread function, resulting in an effective pixel size of 48 μm but an array size of 1 k × 1 k. A reducing fibre-optic taper can be used to lessen the effect of the large point-spread function, but as mentioned earlier, the coupling efficiency will be lower. In addition, the imperfections in tapers will typically introduce a spatial distortion of 2–3% to the image (Faruqi *et al.*, 1999), which will have to be carefully characterized and corrected by image processing if quantitative information is to be extracted from the images. Another problem is that X-rays generated at the scintillator screen, and indeed elsewhere in the TEM, by the high energy electrons can penetrate the fibre-optic plate and reach the CCD, causing bright spots on images. At 400 keV, a 2 k × 2 k CCD camera typically receives 2000 X-ray hits per image with an exposure of 2500 electrons pixel$^{-1}$ (Downing & Hendrickson, 1999). As the intensity of these bright spots due to X-rays has a wide range, removal of them by image processing, particularly from diffraction patterns, is a difficult task. This problem can be easily avoided in a lens coupled system by bending the optical path by 90° (Fig. 6).

While the high collection efficiency offered by a fibre-optic coupler is clearly desirable, particularly for low-dose work, the high photon yield of phosphor screens allows for the use of a less efficient coupler while still maintaining a reasonable sensitivity for the overall imaging system. For the energy range used in TEM, the photon yield of a phosphor screen ranges from a few hundred to a few thousand per incident electron. If 1% of these photons can be relayed to the CCD, a detectable signal will result provided that the CCD has a reasonably high quantum efficiency and a reasonably low noise floor (see section 4.5 below). For example, if 2000 photons are emitted by the scintillating screen for each incident electron, and the collection efficiency of the optical relay is 1%, then 20 photons will reach the CCD. If the CCD has a quantum efficiency of 90%, which is high but achievable, 18 well electrons will be generated in a CCD pixel. If the CCD has a noise floor (include thermal and readout noise) equivalent of 10 well electrons, then the signal due to a single incident electron is statistically detectable. In other words, the system is single-electron sensitive. The parameters used in this analysis are listed in Table 1. Fan & Ellisman (1993) demonstrated this feasibility with a fast two-lens optical relay and a back-side illuminated CCD sensor, but, as is generally the case for a lens relay, the gain in speed is at the expense of resolution. To retain both may require a custom-designed lens that is optimized for a particular optical configuration, such as phosphor emission spectrum, demagnification, field of view, etc. Although the collection efficiency of a typical optical relay is far less than 1%, a custom-designed lens can deliver a collection efficiency of a few percent and maintain a good resolution at the same time. The relatively high collection

**Table 1.** Sensitivity analysis of a CCD imaging system.

| | |
|---|---|
| Electron energy: | 100 keV |
| Scintillator photon yield: | 2000 |
| Optical relay collection efficiency: | 1% |
| Photons reaching CCD: | 20 |
| CCD quantum efficiency: | 90% |
| Signal/incident electron: | 18 $e^-$ |
| Noise floor in CCD: | 10 $e^-$ |

efficiency allows for a thin phosphor screen to be used, which has a better resolution but a low photon yield of less than 500 photons per electron at 400 keV (Fan *et al.*, 2000).

## 4. Imaging system characterization

The following parameters are generally important in characterizing a TEM digital imaging system: resolution, sensitivity, linearity, dynamic range, detection quantum efficiency (DQE) and fixed-pattern noise. Some of these are interdependent, and it is possible and sometimes practised to improve one at the expense of others. This list is not exhaustive, and parameters not listed may also become important depending on the specific application of the imaging system. These have been subject of many publications (De Ruijter & Weiss, 1992; Ishizuka, 1993; Zuo, 1996) and will only be discussed briefly here.

### *4.1. Resolution*

Unlike a general imaging system whose resolution is usually specified in terms of absolute physical dimensions, the resolution of a TEM digital imaging system is specified relative to its array size (Fig. 9). For example, for a 2 k × 2 k imaging system, it is not meaningful to ask what is the smallest specimen detail the imaging system can resolve, as that depends on the TEM's resolution and magnification. Instead, it is more appropriate to ask for the point-spread function, in this 2 k × 2 k array, due to a single incident electron. This will depend on the resolution of the scintillating screen, the optical relay and, indeed, the CCD sensor itself. Resolution can be measured in terms of the point-spread function, e.g. full width at half maximum in number of pixels, or the Fourier transform of it, which is called the modulation transfer function (MTF). Each stage of the imaging chain, i.e. the scintillating screen, the optical relay and the CCD sensor, has its own MTF and the overall MTF of the system is simply the product of all the MTFs of all stages. It is therefore often easier to work with MTF than the point-spread function.

Often, resolution is also expressed in terms of line-spread function, instead of point-spread function, as the line-spread function can be measured directly with the edge test (Dainty & Shaw, 1974). The two functions are related and knowing one allows the other to be derived. The Fourier transform of the line-spread function is also called MTF, although it is different from that derived from the point-spread function.

Two useful methods of measuring the resolution of a TEM CCD imaging system are:

**1** Edge test method (Dainty & Shaw, 1974). A straight metal edge that is thick enough to be opaque to incident electrons can be placed directly above the scintillating screen to measure the resolution of the imaging system

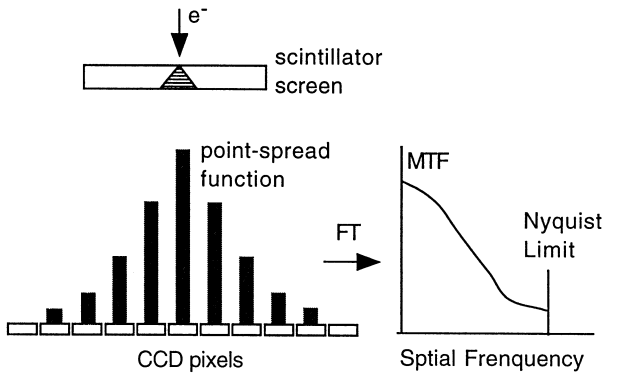


**Fig. 9.** Resolution of a CCD imaging system for TEM. Due to the point-spread function of the system (scintillator screen, optical relay and CCD itself), the signal due to a single incident electron covers several pixels. As a result, the maximum contrast achievable between two adjacent pixels is generally below 20%, as given by the MTF value at the Nyquist limit.

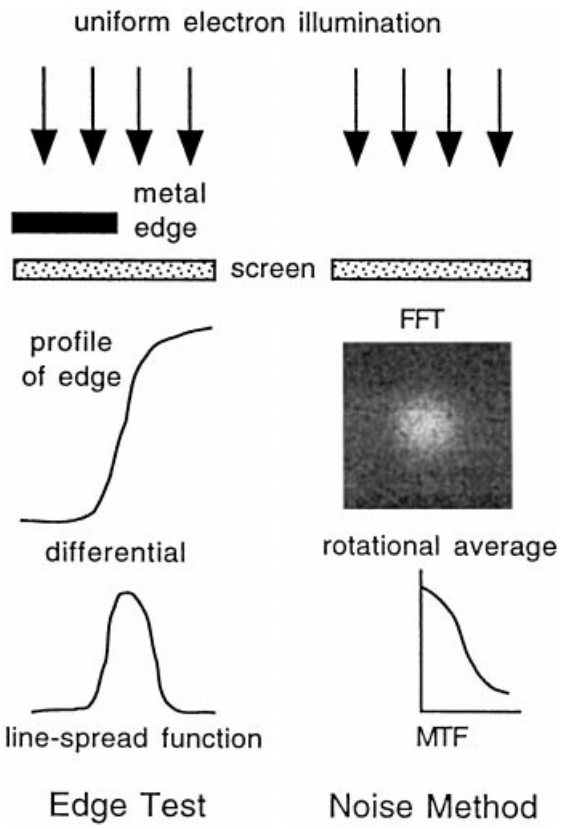


**Fig. 10.** Schematic of two useful methods of measuring resolution of a CCD imaging system: edge test and noise method. In the edge test method, the rise-width (10–90%) of the edge profile function or the full width at half maximum of the line-spread function can be used to characterize the resolution. With the noise method, the MTF can be obtained by rotationally average over the Fourier transform of the image of a uniform illumination.

(Fig. 10). As the edge can be represented as a step function, differentiation of the image of the edge gives the line-spread function of the imaging system. As this function is typically noisy, many lines should be averaged along the edge to reduce noise. The drawback of this method is that the scattering of primary electrons and the generation of secondary electrons around the metal edge may affect the measurement, and the result is generally an over-pessimistic estimate of the MTF.

**2** Noise method (Rabbani *et al.*, 1987; De Ruijter & Weiss, 1992). This method is based on the Fourier analysis of images of a uniform electron illumination (Fig. 10). Due to the fluctuation of the number of electrons landing on a pixel, a uniform illumination actually represents a white noise input, which has a constant power spectrum over all Fourier frequencies. This constant spectrum will be attenuated by the MTF of the imaging system, so the Fourier transform of the image of a uniform illumination gives the MTF of the system (Fig. 10).

Because no special set-up or specimen is required to perform the measurement, this method is very easy to perform and can be done at any time. However, as pointed by Rabbani and co-workers (Rabbani *et al.*, 1987) and more recently by Meyer & Kirkland (1998), the accuracy of this method is influenced by the stochastic scattering of electrons in the scintillating screen, and indeed, the random generation and further scattering of photons in the scintillating screen (Fig. 7). These random processes add noise to the image. As the added noise contains all Fourier frequencies, including high spatial frequencies, this method tends to give an over-optimistic estimate of the MTF. The simulations by Meyer & Kirkland (1998) indicate that the discrepancy is smaller for scintillator screens that do not have a support substrate, such as a thin-foil screen (Fan *et al.*, 1994).

Several other methods of measuring MTF have also been proposed, such as using holographic fringes and amorphous carbon film, but these are not as easy to carry out and have problems of their own, and will not be discussed here.

### 4.2. Sensitivity

This is the minimum detectable signal in terms of the number of incident electrons. If the gain of the system is such that the output signal due to a single incident electron is above the noise floor, as in the example given in Table 1, then the system is single electron-sensitive. Any further boost in gain from this point will not improve the sensitivity but will have, instead, an adverse effect on the dynamic range of the system.

### 4.3. Linearity

This parameter describes the relationship between the output (image intensity in digital units) and the input (number of incident electrons). Although it is true that as long as the two have a fixed and known relationship, which may not be linear, the input can be derived from the output in a quantitative analysis. In practice, however, it is always desirable that the two have a simple relationship, that is, a linear dependence. Due to the nature of CCD sensors described above, its output is strictly linear with the input up to the full well capacity of the CCD. Its linearity is therefore excellent up to the saturation level, provided that the readout circuits do not introduce non-linearities. This is a significant advantage over film, which typically has a more complex response curve (Fig. 11).

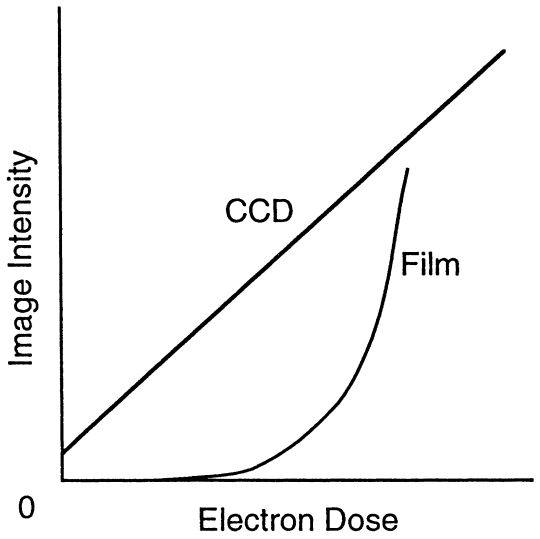


**Fig. 11.** The response of CCD is strictly linear up to the saturation level, whereas that of film is complex and more difficult to characterize.

### 4.4. Dynamic range

This is simply the ratio of the saturation level over the noise floor. In the example given in Table 1, if the full well capacity of the CCD cells is 160 000 $e^-$, then the dynamic range is simply 160 000/10 = 16 000. This quantity is sometimes expressed in units of dB, which is $20*\ln(16000) = 84$ dB in this example. To take full advantage of this dynamic range, an analogue to digital converter of $\log_2(16000) \sim 14$ bits will be required for the system. It is incorrect, however, to assume that the signal quality, as measured by signal-to-noise ratio (SNR), at the output is actually 14 bits, as the SNR of the output can be, at the most, as good as the SNR of the input which is shot-noise limited. The saturation level corresponds to $N = 160\,000/18 \sim 9000$ incident electrons, so the SNR at the input is the square root of $N$, or $\sim 95$ as given by Poisson statistics, which is considerably lower than 14 bits. This gives an upper limit to the SNR at the output. To find

out the actual SNR at the output, the following parameter is required.

### 4.5. Detection quantum efficiency (DQE)

DQE characterizes the noise performance of an imaging system, and is defined as (Herrmann & Krahl, 1982):

$$\mathrm{DQE} = [(\mathrm{SNR})_o/(\mathrm{SNR})_i]^2 \quad (1)$$

where $(\mathrm{SNR})_o$ and $(\mathrm{SNR})_i$ are the signal-to-noise ratio at the output and input, respectively.

For an ideal system, DQE should be unity, which means that the system itself is noise free. In practice, of course, a system always contributes a certain amount of noise, so its DQE is always less than unity. The main sources of noise in a CCD-based TEM digital imaging system are: readout noise from the electronics (amplification, A/D conversion, etc.), thermal noise in the CCD and pulse-width distribution in the scintillating screen. Readout noise is at a fixed level, meaning it is independent of the integration time or electron dose. It is likely to be the dominant noise for low dose imaging conditions. Thermal noise is due to thermal excitations in CCDs, as discussed earlier, and the resulting dark noise accumulates with time. It can be reduced by cooling the CCD, and is lowered by 50% for every 7 °C drop in temperature of the CCD sensor. As thermal noise accumulates with time, it is likely to be the dominate noise for long integration times. The pulse width distribution reflects the fact that the electron–photon conversion in the scintillator is a random process, and the number of photons generated due to each incident electron is not a constant but follows a probability distribution called pulse-width distribution. Thus, even if the readout noise and thermal noise could be completely eliminated from the CCD, system DQE would not be unity simply because of this conversion process. This type of noise can be reduced by selecting a scintillating material that has a narrower pulse width distribution. Crystalline YAG screens, for example, are generally better than powder phosphor screens in this respect.

DQE can be measured if the overall gain of the system is calibrated, that is, if the pixel intensity change due to a single incident electron is known. Supposing one incident electron causes a pixel intensity increase, on the average, of $g$ digital units, which can be greater or smaller than 1. With a uniform electron illumination, the average number of electrons per pixel, $N$, can be calculated from the image mean, $M$, by

$$N = M/g, \quad (2)$$

and for a Poisson process

$$(\mathrm{SNR})_i = N^{1/2}. \quad (3)$$

The standard deviation ($\sigma$) of the image can also be measured, so $(\mathrm{SNR})_o$ can be calculated easily:

$$(\mathrm{SNR})_o = M/\sigma. \quad (4)$$

From (Eqs 1–4), we have:

$$\mathrm{DQE} = M^*g/\sigma^2. \quad (5)$$

However, actual measurements will invariably yield a DQE that is considerably greater than 1. This is due to the convolution effect of the point-spread function of the imaging system which causes cross-talk between pixels, or channel mixing. Any pixel therefore receives contributions from its neighbouring pixels as a result. This problem has been addressed by de Ruijter & Weiss (1992) and Ishizuka (1993). In effect, this convolution effect improves the 'apparent' DQE but at the expense of resolution. Ishizuka (1993) has devised a method for measuring DQE based on curve-fitting of measured image variance as a function of electron dose, and more details can be found there.

DQE is a function of electron dose. At low dose levels of a few incident electrons pixel$^{-1}$, DQE of a TEM CCD imaging system is typical low (Fig. 12) due to the readout noise of CCD, but it improves rapidly with electron dose to a stable level. At dose levels of 100 electrons per pixel and higher, the improvement of DQE with electron dose becomes insignificant.

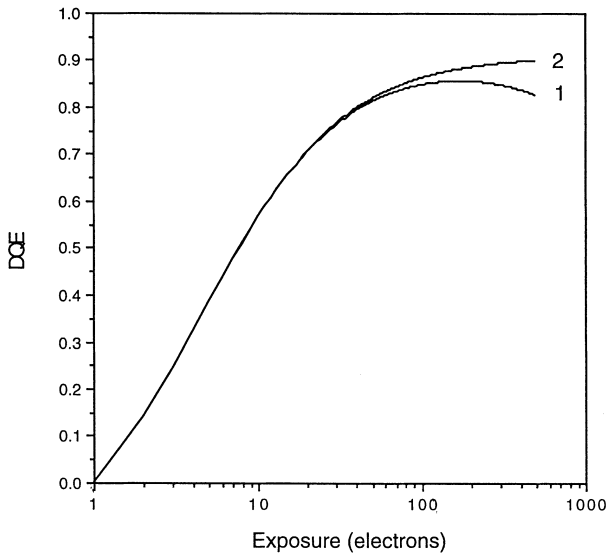


**Fig. 12.** DQE of a CCD imaging system for TEM is typically low at low dose levels due to the readout noise in the CCD electronics, but increases rapidly with dose and plateaus at the dose level of ~100 electrons pixel$^{-1}$. DQE goes down at higher dose levels if gain-normalization of images is not done properly (curve 1). DQE approaches a constant (curve 2) if the gain reference (flat field) and dark noise images used for gain-normalization, obtained with a uniform illumination and no illumination, respectively, are averaged over many frames to avoid gain variations.

### *4.6. Fixed-pattern noise*

Another unique aspect of large format CCD imaging systems is that, owing to the large number of pixels contained in a CCD sensor, some defects are unavoidable even in the highest grade CCDs. These defects include individual or groups of pixels having an abnormal response, i.e. they may have a higher level of dark noise, or may be brighter or dimmer than the rest of the pixels under a uniform illumination. These give rise to a fixed-pattern noise in an image. In addition, the non-uniformity in the scintillator screen, defects in the fibre-optic coupler (which often form chicken-wire patterns) or vignetting of the lens relay also contribute to the fixed-pattern noise. Fortunately, this problem can be very effectively corrected by a simple gain-normalization procedure. This involves acquiring a dark noise image (with no illumination), denoted by $D$, and an image of a uniform illumination, denoted by $G$, which are used as the gain reference (sometimes called flat-field). Then a raw image, denoted by $I_r$, can be gain-normalized to yield the correct image, denoted by $I$, by applying a pixel-wise operation given by:

$$I = C^*(I_r - D)/(G - D) \quad (6)$$

where $C$ is a constant and should be set to be the mean of $(G - D)$ to preserve image intensity. To avoid fluctuations in the dark noise image and in the gain reference, both $D$ and $G$ should be averaged over many frames before using. Not doing so will degrade the DQE of the system (Fig. 12), particularly at high electron dose (Ishizuka, 1993).

## 5. Other developments and future challenges

### *5.1 Application-specific integrated circuit-based electron detectors*

The main restriction of CCDs in TEM applications is that they cannot be used directly in the electron beam. The conversion process, from electrons to photons, degrades resolution, sensitivity and DQE of CCD-based imaging systems. Fan and co-workers (Fan *et al.*, 1998) recently demonstrated the feasibility of a potential alternative to CCD technologies for TEM digital imaging, namely, two-dimensional electron detectors based on the application-specific integrated circuit (ASIC, Fig. 13). This type of detector has characteristics that are markedly different from those of CCDs: (1) they can be used directly under electron bombardment (energy range tested: 20–400 keV), therefore require no scintillator screen; (2) each pixel of the device is an electron counter and generates digital output independently; (3) the readout of the device is frameless and event-driven; (4) the device can be operated at room temperature and is nearly noise free; and (5) the counting dynamic range of the device is virtually unlimited.

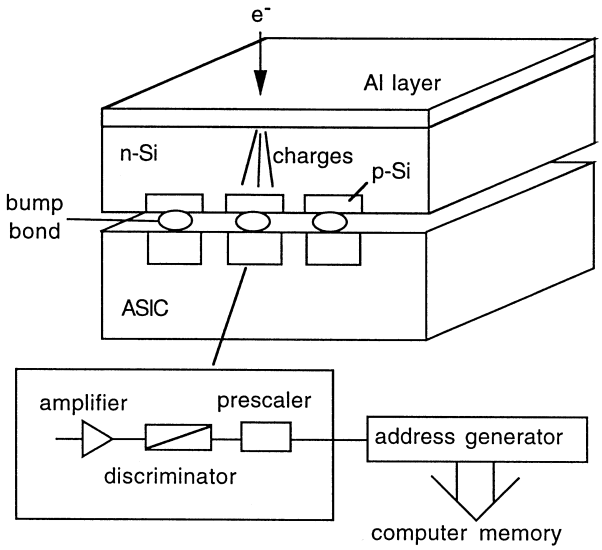


**Fig. 13.** Each pixel in an ASIC-based detector is an electron counter, which can update (via the address generator) a computer memory location mapped to the pixel when a single event or a specified number of events, depending on the setting of the prescaler, have been detected.

In essence, each pixel of the 2D detector is an event-driven counter (Fig. 13) that can be programmed to report a single event (electron landing) or a specified number of events. Each pixel is mapped to a computer memory location, which will be updated automatically when the pre-specified number of events has occurred at the corresponding pixel. No active readout of the 2D device is needed, so the device can be in counting mode continuously and the accumulated image can be monitored in the meantime. The extremely large signal from each high energy electron allows the threshold of the discriminator (Fig. 13) to be set high enough that false pulses due to thermal noise in the Si will not trigger the counter. Unlike CCDs, whose dynamic range is limited by their full well capacity, an ASIC-based detector has virtually unlimited counting dynamic range.

The limitations of this type of device are: (1) the extremely high overall counting rate even with a modest array size, say, 1 k × 1 k will impose too high a burden on the host computer, and (2) multiple counting of a single event by neighbouring pixels. For the 8 × 8 device tested (Fan *et al.*, 1998) the maximum counting rate is ~ 1 MHz pixel$^{-1}$, which in itself is not a limitation. However, for a usable device of 1 k × 1 k pixels, the overall event rate will be unmanageable if all pixels operate near the maximum pixel rate. Even at an average counting rate of 1 kHz pixel$^{-1}$, the overall counting rate will be 1 GHz, which is beyond what can be handled by a PC at the present time. However, for a point- or one-dimensional electron detector, or a 2D detector for low dose applications, the

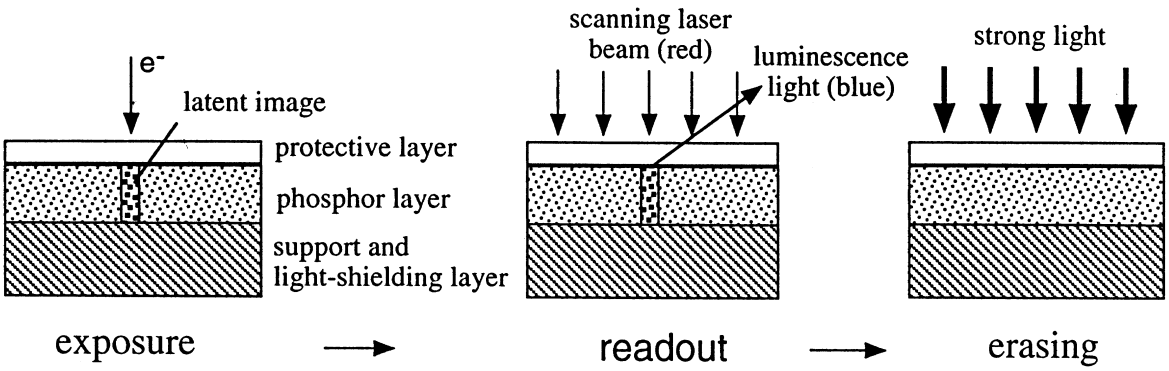


**Fig. 14.** Schematic structure and operation of the 'imaging plate'. A latent image is created on the imaging plate by incident electrons, which is readout (digitized) with a scanning laser beam in a 'reader'. Compared with film, the imaging plate offers a much larger dynamic range, good sensitivity and excellent linearity, but the resolution is not as good. Like film, the imaging plate also requires off-line processing before an image is available.

ASIC-based detector makes good sense. Multiple counting of a single event by neighbouring pixels is a result of a finite point-spread function of the system, but can be reduced or even eliminated by a more elaborate circuit design, as has been suggested by Fan *et al.* (1998).

### 5.2. *'Imaging plate'*

The 'imaging plate' (Fig. 14) for TEM imaging was jointly developed by Fuji Film and JEOL (see, e.g. Mori *et al.*, 1988; Isoda *et al.*, 1991; Zuo *et al.*, 1996). Its principle and operation are illustrated in Fig. 14. It has the same physical dimension (96.6 mm × 80.9 mm) as the commonly used TEM film and is compatible with the existing film camera on most transmission electron microscopes without modification. However, a separate off-line reader is required to digitize the latent image formed on an imaging plate. Compared with film, the imaging plate has an excellent linearity, very large dynamic range, good sensitivity (Isoda *et al.*, 1991) and a DQE better than that of the CCD at low dose (Zuo *et al.*, 1996). Its resolution, however, is considerably worse than film. Using a 25 μm or 50 μm aperture on the reader, an imaging plate can provide an image with 3760 × 3000 or 1880 × 1500 pixels, respectively. The main limitation, however, is that the image captured on an imaging plate is not available on-line, as the imaging plates must be removed from the microscope and processed (readout and erased) off-line on a reader (Fig. 14) before the image can be displayed or analysed.

### 5.3. *Multiport readout CCDs*

Current CCD imaging systems surpass film in nearly all important aspects. A major drawback, however, is that they do not provide enough pixels; at the present (Fig. 2) the largest available CCD imaging system for TEM has 2 k × 2 k pixels. That is about one order of magnitude smaller than can be provided by a piece of TEM film, which, when digitized properly, can provide ~ 7 k × 7 k pixels or more. A comparable CCD array will be needed to match the large field of view and the large details typically contained in a piece of TEM film with which many microscopists have become familiar. This is perhaps the most important reason why film recording is still widely used in TEM today.

Future CCD imaging systems with this kind of array size offer several challenges. For example, one image takes ~ 100 MB of data, assuming each pixel takes 2 bytes, as is typical in current CCD imaging systems, and a tomographic series containing 61 tilts will take more than 6 GB storage space. Processing and transferring data packages of this size are non-trivial tasks for the current PC-based imaging systems. Also, reading a 7 k × 7 k image off the CCD (digitizing the charges collected in the CCD cells) alone takes 49 s using a readout speed of 1 MHz. The demand on CCD charge transfer efficiency will also be higher due to the large number of transfers.

One approach that avoids these problems is to implement multiport parallel readout on-chip, which increases the readout speed and reduces the number of transfers at the same time. Fan and co-workers (Fan *et al.*, 2000) have recent developed a 5 megapixel (2.5 k × 2 k) CCD imaging system for TEM applications based on a multiport readout, frame transfer CCD sensor (Fig. 15). This system makes use of four of the eight on-chip parallel readout ports, and achieves a total readout speed of 4 MHz without increasing the readout noise. With a lens relay that is specifically designed for the application, this system achieves single electron sensitivity at 400 keV and a MTF value of 14% at the Nyquist frequency, measured using the noise method. As pointed out earlier in this paper, the noise method generally gives an over-optimistic estimate of the of MTF but, as the simulations by Meyer & Kirkland (1998) show, the discrepancy is small for the thin-foil based screens at 400 keV. Regardless of the actual value of MTF at the

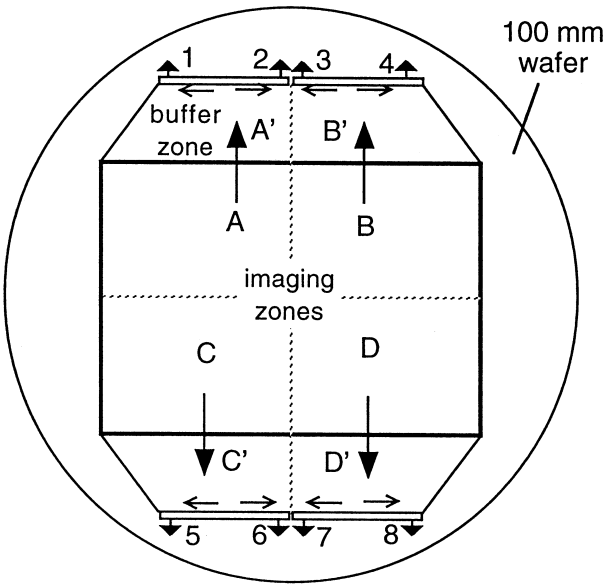


**Fig. 15.** For large format CCDs, multiport readout design offers faster frame rate, less image smearing and less charge loss due to fewer and shorter charge transfers.

Nyquist frequency, as long as it is significantly above the noise level, information can, at least in theory, be recovered all the way to the Nyquist limit by using appropriate deconvolution algorithms.

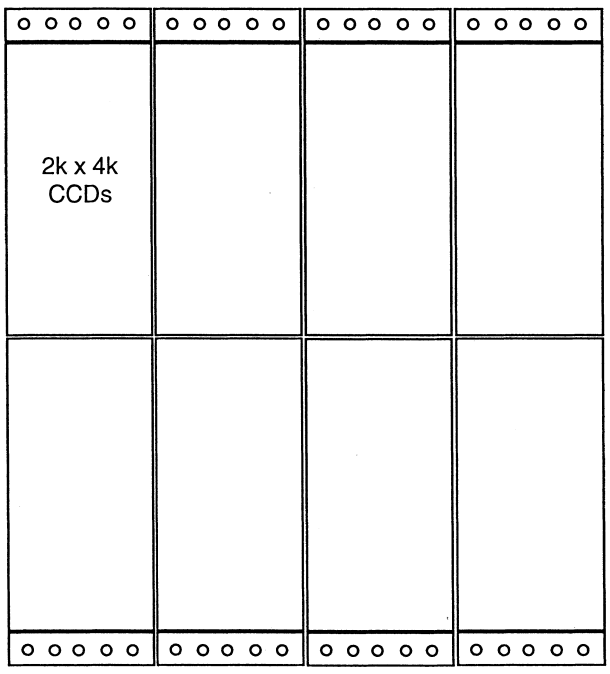


**Fig. 16.** Three-side abuttable CCDs can be assembled to form a very large composite CCD. However, the inevitable gaps between individual CCDs cause complications and may limit the applications of this type of composite device in TEM imaging.

### *5.4. Abuttable CCDs*

The multiport readout CCD sensor described above takes an entire 100 mm diameter silicon wafer. For even larger devices, individual CCD sensors can be assembled in a mosaic arrangement (Fig. 16). Three-side abuttable CCDs have been developed for astronomy applications (Burke *et al.*, 1998), in which each CCD has 2 k × 4 k pixels, and a pixel size of 15 μm. Using these 2 k × 4 k abuttable CCDs, 8 k × 8 k (or larger in one direction, e.g. 8 k × 10 k) composite CCDs can be constructed (Burke *et al.*, 1998), which would be adequate for TEM applications. However, there are inevitable gaps, in the order of a few hundred micrometres at present, between the CCDs in these composite devices, which means that there are missing strips in images captured by them. Although there are ways of dealing with the missing data problem, they will make the system more complicated to operate. The usefulness of such composite devices for TEM imaging is yet to be seen.

## 6. Concluding remarks

Digital imaging in transmission electron microscopy has come a long way in meeting the high demands of recording high resolution images and large dynamic range diffraction patterns. CCD-based large format digital imaging systems have become practical for many TEM applications, and provide numerous advantages over film recording, including higher sensitivity, larger dynamic range, better linearity, lower noise and immediate image access. However, further development will be needed for these systems to match the resolution and information content provided by a typical TEM negative. This is by no means a trivial task, as it in fact challenges several fields including CCD, electron scintillator, optical relay and computer technologies.

## Acknowledgements

This work is supported by NIH grant RR-04050 and NSF grant ASC 9318180.

## References

Aikens, R.S., Agard, D.A. & Sedat, J.W. (1989) Solid state imagers for microscopy. *Methods Cell Biol.* **29**, 291–313.

Boyle, W.S. & Smith, G.E. (1970) Charge-coupled semiconductor devices. *Bell Systems Tech. J.* **49**, 587–599.

Brink, J. & Chiu, W. (1994) Applications of a slow-scan CCD camera in protein electron crystallography. *J. Struct. Biol.* **113**, 23–34.

Burke, B.E., Gregory, J.A., Mountain, R.W., Kosicki, B.B., Savoye, E.D., Daniels, P.J., Dolat, V.S., Lind, T.L., Loomis, A.H., Young, D.J., Luppino, G.A. & Tonry, J.L. (1998) Large-area back-illuminated CCD imager development. *Exp. Astron.* **8**, 31–40.

Chapman, J.N., Craven, A.J. & Scott, C.P. (1989) Electron detection

in the analytical electron microscope. *Ultramicroscopy*, **28**, 108–117.

Daberkow, I., Herrmann, K.-H., Liu, L. & Rau, W.D. (1991) Performance of electron image converters with YAG single-crystal screen and CCD sensor. *Ultramicroscopy*, **38**, 215–223.

Daberkow, I., Herrmann, K.-H., Liu, L., Rau, W.D. & Tietz, H. (1996) Development and performance of a fast fiber-plate coupled CCD camera at medium energy and image processing system for electron holography. *Ultramicroscopy*, **64**, 35–43.

Dainty, J.D. & Shaw, R. (1974) *Image Science.* Academic Press Inc, New York.

De Ruijter, W.J. & Weiss, J.K. (1992) Method to measure properties of slow-scan CCD cameras for electron microscopy. *Rev. Sci. Instrum.* **63**, 4314–4321.

Dierksen, K., Typke, D., Hegerl, R., Koster, A.J. & Baumeister, W. (1992) Towards automatic electron tomography. *Ultramicroscopy*, **40**, 71–87.

Downing, K.H. & Hendrickson, F.M. (1999) Performance of a 2k CCD camera designed for electron crystallography at 400 kV. *Ultramicroscopy*, **75**, 215–233.

Duan, X.F., Gao, M. & Peng, L.-M. (1998) Accurate measurement of phase shift in electron holography. *Appl. Phys. Lett.* **72**, 771–773.

Fan, G.Y., Datte, P., Beuville, E., Beche, J.-F., Millaud, J., Downing, K.H., Burkard, F.T., Ellisman, M.H. & Xuong, N.-H. (1998) ASIC-based event-driven 2D digital electron counter for TEM imaging. *Ultramicroscopy*, **70**, 107–113.

Fan, G.Y., Dunkelberger, D.G. & Ellisman, M.H. (1994) Performance of thin foil scintillating screen for transmission electron microscopy. *Ultramicroscopy*, **55**, 7–14.

Fan, G.Y. & Ellisman, M.H. (1993) High-sensitivity lens coupled slow-scan CCD camera for transmission electron microscopy. *Ultramicroscopy*, **52**, 21–29.

Fan, G.Y. & Ellisman, M.H. (1996) Optimization of thin-foil based phosphor screens for CCD imaging in TEM in the voltage range of 80–400 kV. *Ultramicroscopy*, **66**, 11–19.

Fan, G.Y., Peltier, S., Lamont, S., Dunkelberger, D.G. & Ellisman, M.H. (2000) Multiport-readout frame-transfer 5 megapixel CCD imaging system for TEM applications. *Ultramicroscopy*, **84**, 75–84.

Fan, G.Y., Young, S.J., Mercurio, P.J. & Ellisman, M.H. (1993) Telemicroscopy. *Ultramicroscopy*, **52**, 499–503.

Faruqi, A.R., Andrews, H.N. & Henderson, R. (1995) A high sensitive imaging detector for electron microscopy. *Nucl. Instrum. Meth. Phys. Res. A*, **367**, 408–412.

Faruqi, A.R., Henderson, R. & Subramaniam, S. (1999) Cooled CCD detector with tapered fiber optics for recording electron diffraction patterns. *Ultramicroscopy*, **75**, 253–270.

Fiebiger, J.R. & Muller, R.S. (1972) Pair-production energies in silicon and germanium bombarded with low energy electrons. *J. Appl. Phys.* **43**, 3202–3207.

Herrmann, K.-H. & Krahl, D. (1982) The detection quantum efficiency of electronic image recording systems. *J. Microsc.* **127**, 17–28.

Herrmann, K.-H. & Liu, L. (1992) Performance of image converters using slow-scan CCDs in MeV electron microscopy. *Optik*, **92** (2),48–50.

Herrmann, K.-H. & Sikeler, R. (1995) Low-energy electron image converters for high resolution slow-scan CCD sensor. *Optik*, **98**, 119–124.

Ishizuka, K. (1993) Analysis of electron image detection efficiency of slow-scan CCD cameras. *Ultramicroscopy*, **52**, 7–20.

Isoda, S., Saitoh, K., Moriguchi, S. & Kobayashi, T. (1991) Utility test of imaging plate as a high-resolution image-recording material for radiation-sensitive specimens. *Ultramicroscopy*, **35**, 329–338.

Joy, D.C. (1988) An introduction to Monte Carlo simulations. *Inst. Phys. Conf Ser*, **93**(1), 23–32.

Koster, A.J., Chen, H., Sedat, J.W. & Agard, D.A. (1992) Automated microscopy for electron tomography. *Ultramicroscopy*, **46**, 207–227.

Koster, A.J. & de Ruijter, W.J. (1992) Practical autoalignment of transmission electron microscopes. *Ultramicroscopy*, **40**, 89–95.

Krivanek, O.L. & Fan, G.Y. (1992) Application of slow-scan CCD cameras to on-line microscope control. *Scanning Microscopy Supplement*, **6**, 105–114.

Krivanek, O.L. & Mooney, P.E. (1993) Applications of slow-scan CCD cameras in transmission electron microscopy. *Ultramicroscopy*, **49**, 95–108.

Krivanek, O.L., Mooney, P.E. & Fan, G.Y. (1991) Slow-scan CCD camera for transmission electron microscopy. *Inst. Phys. Conf Ser*, **119**(119), 523–526.

Kujawa, S. & Krahl, D. (1992) Performance of a low-noise CCD camera adapted to a transmission electron microscope. *Ultramicroscopy*, **46**, 395–403.

Meyer, R.R. & Kirkland, A. (1998) The effect of electron and photon scattering on signal and noise transfer properties of scintillators in CCD cameras used for electron detection. *Ultramicroscopy*, **75**, 23–33.

Mori, N., Oikawa, T., Katoh, T., Miyahara, J. & Harada, Y. (1988) Application of the 'imaging plate' to TEM image recording. *Ultramicroscopy*, **25**, 195–202.

Rabbani, M., Shaw, R. & Van Metter, R. (1987) Detective quantum efficiency of imaging systems with amplifying and scattering mechanisms. *J. Opt. Soc. Am. A*, **6**, 1156–1164.

Roberts, P.T.E., Chapman, J.N. & MacLeod, A.M. (1982) A CCD-based image recording system for the CTEM. *Ultramicroscopy*, **8**, 385–396.

Russ, J.C., Radzimski, Z.J., Buczkowski, A. & Maynard, L. (1990) Monte-Carlo modeling of electron signals from heterogenous specimens with nonplanar surfaces. *J. Comp. Assist. Microsc.* **2** (2),59–76.

Spence, J.C.H. & Zuo, J.M. (1988) Large dynamic range, parallel detection system for electron diffraction and imaging. *Rev. Sci. Instrum.* **59**(9), 2102–2105.

Theuwissen, A.J.P. (1995) *Solid-State Imaging with Charge-Coupled Devices.* Kluwer Academic Publishers, Dordrecht.

Voelkl, E., Allard, L.F., Nolan, T.A., Hill, D. & Lehmann, M. (1997) Remote operation of electron microscopes. *Scanning*, **19**, 286–291.

Zuo, J.M. (1996) Electron detection characteristics of slow-scan CCD camera. *Ultramicroscopy*, **66**, 21–33.

Zuo, J.M., McCartney, M.R. & Spence, J.C.H. (1996) Performance of imaging plates for electron recording. *Ultramicroscopy*, **66**, 35–47.